A low-background $\gamma\gamma$-coincidence spectrometer for radioisotope studies

Andrew Tillett [a], John Dermigny [a,b], Mark Emamian [b,c], Yuri Tonin [a,f], Igal Bucay [a], Rachel L. Smith [d,e], Michael Darken [a], Corey Dearing [a], Mikaela Orbon [a], Christian Iliadis [a,b,*]

[a] Department of Physics and Astronomy, The University of North Carolina at Chapel Hill, Chapel Hill, NC 27599, USA
[b] Triangle Universities Nuclear Laboratory (TUNL), Durham, NC 27708, USA
[c] Department of Physics, Duke University, Durham, NC 27708, USA
[d] North Carolina Museum of Natural Sciences, 121 West Jones Street, Raleigh, NC 27603, USA
[e] Department of Physics and Astronomy, Appalachian State University, 525 Rivers Street, Boone, NC 28608-2106, USA
[f] CAPES Foundation, Ministry of Education of Brazil, Brasília, DF, 70.040-020, Brazil

ARTICLE INFO

MSC 2010:
00-01
99-00

Keywords:
elsarticle.cls
LaTeX
Elsevier
Template

ABSTRACT

The performance of a new, low-background NaI(Tl) spectrometer, based on $\gamma\gamma$-coincidence counting, is discussed. We present experimental coincidence efficiencies, timing resolutions, background count rates, and minimum detectable activities. The spectrometer has been simulated using Geant4, and the results are used for estimating coincidence efficiencies for volume sources. To test the device, we measured the cosmogenic ^{26}Al activity in a small (17.7 g) meteorite fragment. We find a value of 52.9 ± 7.8 dpm/kg, in agreement with the activity measured previously in a much larger fragment of the same meteorite using a HPGe detector.

1. Introduction

Gamma-ray spectroscopy allows for the measurement of radioisotope concentrations without destroying the samples. The coincident detection of γ-rays is of particular interest because it improves significantly the signal-to-background ratio. Since more than one radiation detector is involved in these measurements, the method is also referred to as multi-dimensional γ-ray spectrometry. The smallest multi-dimensional spectrometer consists of two detectors. Such systems have been discussed before [1–8]. However, the complete performance of a $\gamma\gamma$ coincidence spectrometer in terms of coincidence efficiencies, timing resolutions, background count rates, and detection sensitivity has rarely been reported.

We will discuss an instrument that was recently commissioned at The University of North Carolina at Chapel Hill. It was built for assaying atmospheric, environmental, and extraterrestrial samples. We will describe the performance of the new spectrometer and, in particular, will focus on the detection of ^{22}Na, ^{26}Al, and ^{60}Co. The instrument was tested by measuring the concentration of ^{26}Al in a small meteorite fragment of the Farmville meteorite. The $\gamma\gamma$-coincidence spectrometer is described in Section 2. Measurements and results are discussed in Section 3. Conclusions are presented in Section 4.

2. Equipment

The spectrometer is shown in Figs. 1 and 2. It consisted of two NaI(Tl) detectors, purchased from Saint-Gobain Crystals/Bicron (Newbury, OH, USA), which faced each other at a distance of 38.1 mm along their symmetry axis. Each detector contained a crystal with a diameter of 152.4 mm and length of 101.6 mm, inside an aluminum housing with a wall thickness of 0.81 mm. The crystals were coupled to a photomultiplier tube (PMT) of 127.0-mm diameter via a low-background optical quartz window. The only spectrometer part selected for low-background radiation was the optical window.

The detectors were surrounded by several layers of different metals. The innermost layer consisted of 0.64-cm thick copper, surrounded by 10.2-cm thick lead. The outermost layer was made of 1.0-cm thick aluminum and provides support for the shielding above the detectors. The top shield consisted of a WWII (low-background) steel plate of 2.0-cm thickness, which supported a 10.2-cm-thick layer of lead bricks and another 2.0-cm-thick steel plate. A 10.2-cm-diameter hole at the center of the top shield provided convenient access to the sample located between the two detectors.

A lead plate of 2.54-cm thickness was located between the detector front faces to reduce background coincidence events caused by the

* Corresponding author.
E-mail address: iliadis@unc.edu (C. Iliadis).

http://dx.doi.org/10.1016/j.nima.2017.07.057
Received 19 June 2017; Received in revised form 25 July 2017; Accepted 27 July 2017
Available online 5 August 2017

Fig. 1. (Color online) The $\gamma\gamma$-coincidence spectrometer consisted of two NaI(Tl) detectors inside a passive shield. The top shield, made of steel and lead, was removed to show the detector geometry.

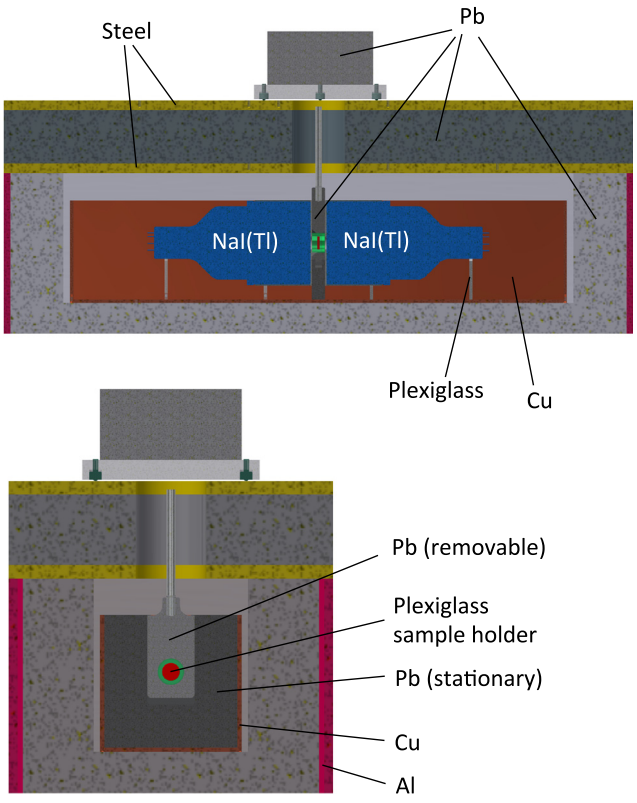

Fig. 2. (Color online) Cross-sectional views of the $\gamma\gamma$-coincidence spectrometer, showing the geometry and the different layers of materials. Part of the lead shield, located between the two detectors (see lower panel), was removable and contained the sample holder made of plexiglass.

Compton scattering of γ-rays between the detectors. Background radiation was reduced by a factor of two to four by this shield, depending on the coincidence gate used (Section 3.2). This lead plate had a central hole of 3.8-cm diameter, with tapered edges to reduce the absorption of

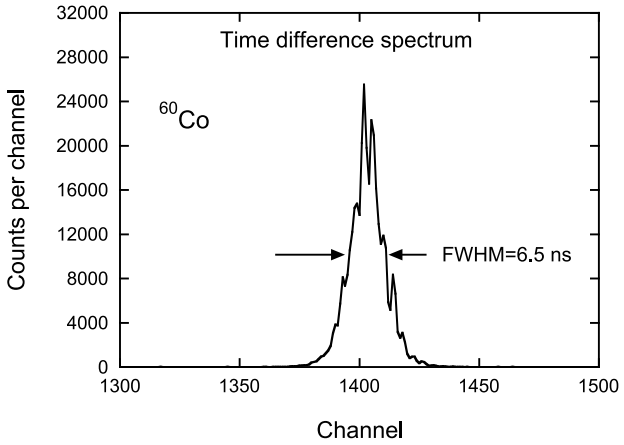

Fig. 3. Timing spectrum of the NaI(Tl) $\gamma\gamma$-coincidence spectrometer, measured using a ^{60}Co calibration source. A 13-ns wide software gate around this peak defined a coincidence event between the two detectors. Additional coincidence gates were applied to certain energy regions (see text).

γ-rays originating from the sample. The sample holder was made of 1.5-mm-thick plexiglass and could be conveniently inserted into the central hole of the lead plate (see lower panel of Fig. 2).

The detectors were biased with a voltage of +850 V. The output signal from each detector was split into two branches without pre-amplification. The first signal was processed by a spectroscopy amplifier with 0.5-μs shaping time and was subsequently fed into a 4096-channel VME amplitude-to-digital converter (ADC). The second signal was processed by a fast timing filter amplifier (TFA) with 50-ns integration and differentiation time constants, and was then fed into a constant-fraction discriminator (CFD) with a 64-ns shaping delay. The logic output signal provided the gate for the ADC and the start and stop signals for the time-to-amplitude converters (TAC). The output of the TAC was also fed into the ADC. The data were stored in list mode for subsequent offline analysis, where each event consists of the energy and timing information for both detectors. All timing and energy coincidence gating was performed using the data acquisition system JAM [9].

3. Performance

3.1. Calibration sources

A ^{60}Co calibration source was used to determine the energy and timing resolutions. The energy resolutions amounted to 5.1% at 1333 keV for both detectors. The timing spectrum obtained with detector 1 starting and detector 2 stopping the TAC is shown in Fig. 3. The time resolution, defined as the full width at half maximum (FWHM) of the peak, amounted to 6.5 ns. A software gate of 13 ns covered the timing peak and defined a coincidence event, and was applied to all coincidence spectra presented here. Additional software gates were applied to certain energy regions, as discussed below.

Fig. 4 shows two-dimensional histograms of the energy deposited in detector 2 versus the energy deposited in detector 1. The top and bottom panels were obtained using a ^{22}Na and ^{60}Co calibration source, respectively, located in the center of the spectrometer.

The radioisotope ^{22}Na has a half-life of $T_{1/2} = 2.6029 \pm 0.0008$ yr and decays predominantly by positron emission to the first excited state of ^{22}Ne.[1] For 100 decaying ^{22}Na nuclei, 99.94 ± 0.13 photons of 1274.5 keV energy and 180.7 ± 0.2 photons of 511.0-keV energy are emitted. The two-dimensional histogram in the top panel of Fig. 4 displays regions

[1] The half-lives and branching ratios quoted in the present work are adopted from the Laboratoire National Henri Becquerel; see http://www.nucleide.org/DDEP_WG/DDEPdata.htm.

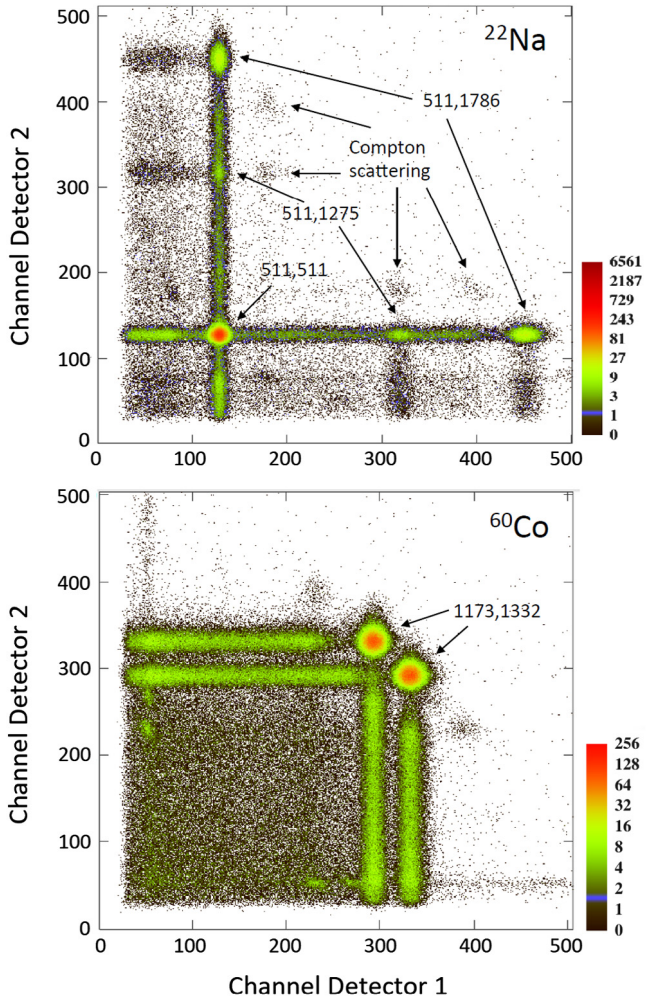

Fig. 4. (Color online) Two-dimensional histograms of energy deposited in detector 2 versus energy deposited in detector 1, measured using a ^{22}Na (top panel) and ^{60}Co (bottom panel) calibration source. The values in the panels indicate γ-ray energies in units of keV. The notation "511, 511" refers to the detection of one 511 keV photon in one counter and of the other 511 keV photon in the other counter.

of different coincidence events, depending on which and how many of the simultaneously emitted photons are detected in the spectrometer. The highest intensity region (lower left) corresponds to one 511-keV photon depositing its energy in the first detector and the other 511 keV in the second detector (labeled by "511, 511"). Two regions correspond to a 511 keV photon detected in one counter and a 1275-keV photon in the other counter ("511, 1275"). Finally, two other regions correspond to one 511 keV photon depositing its energy in one detector and the other 511-keV photon together with the 1275-keV photon in the other detector ("511, 1786"). Since the two detectors are relatively large and are located in close geometry, the region of the 511, 1786 coincidences has a much higher intensity compared to the region of the 511, 1275 coincidences. Similar results have been reported in Ref. [5].

The radioisotope ^{60}Co has a half-life of $T_{1/2} = 5.2711 \pm 0.0008$ yr and decays by β^- emission predominantly to the third excited state in ^{60}Ni. For 100 decaying ^{60}Co nuclei, 99.85 ± 0.03 photons of 1173.2-keV energy and 99.9826 ± 0.0006 photons of 1332.4-keV energy are emitted. The two regions corresponding to one of these photons depositing its energy in one detector and the other photon in the other detector are labeled "1173, 1332" in the bottom panel of Fig. 4.

Tight coincidence gates ("energy cuts") can be set around the regions of interest in Fig. 4. The events inside any two-dimensional gate were projected onto the horizontal (energy of detector 1) and vertical

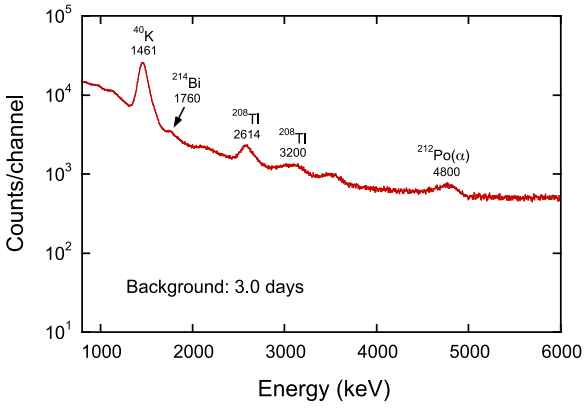

Fig. 5. (Color online) Background spectrum measured with one NaI(Tl) detector in singles mode for a period of 3.0 days. A large fraction of the observed background radiation (^{40}K, ^{214}Bi, ^{208}Tl, and ^{212}Po) is most likely caused by internal contributions from the glass and ceramic insulator of the photomultiplier tube, and from the crystal itself.

(energy of detector 2) axes and the resulting pulse-height spectra were summed to produce a composite one-dimensional histogram for count rate estimates.

Detection efficiencies for the main peaks discussed above are listed in Table 1. We define the peak efficiency as the ratio of the net intensity of a given peak and the total number of decaying nuclei (^{22}Na or ^{60}Co) during the measurement period. The ^{22}Na and ^{60}Co point-like sources had certified activities of 20.9 Bq and 1090 Bq, respectively, at the time of measurement. Singles efficiencies are listed for detector 1 only and are twice as large for the entire spectrometer. Coincidence efficiencies are obtained by setting tight energy gates on the coincidence regions discussed above. The efficiency for 511, 511 coincidences is about 12%. However, these events are common for all β^+ emitters and thus do not distinguish between different positron-emitting radionuclides (e.g., ^{22}Na and ^{26}Al) in a mixed sample. Coincidences involving the characteristic γ-rays, e.g., the energy sum $511 + 1275$ keV $= 1786$ keV for ^{22}Na, or the 1172 keV and 1332 keV γ-rays for ^{60}Co, result in detection efficiencies of about 2.6%–5.2%.

3.2. Background radiation and minimum detectable activities

The background radiation consisted of external (i.e., from outside the radiation shield and the shield itself) and internal (i.e., detector crystals and assembly) contributions. A background spectrum, measured using one of the detectors in singles mode over a time period of 3 days, is shown in Fig. 5. The peaks at 1461 keV and 1760 keV originate from ^{40}K and ^{214}Bi, respectively. Two other peaks arise from ^{208}Tl. For 100 decays of this nuclide, 99.755 ± 0.004, 85.0 ± 0.3, and 22.5 ± 0.2 photons of energy 2614.5 keV, 583.2 keV, and 510.7 keV, respectively, are emitted. It is worth noting that the third γ-ray has incidentally the same energy as the 511 keV annihilation radiation. A significant fraction of decays results in the two-photon cascade $583 + 2614$ keV, and to a lesser degree, in the three-photon cascade $511 + 583 + 2614$ keV. The observation of the sum peak near $583 + 2614$ keV ≈ 3200 keV in Fig. 5 hints at a very close proximity of the ^{208}Tl source to the crystal. A large fraction of the observed ^{208}Tl and ^{40}K decays originates presumably from the glass and the ceramic insulators of the photomultiplier tubes [10]. The peak near 4800 keV is most likely caused by a small Th/U contamination of the NaI crystal itself, specifically from the emission of α-particles in the decay of ^{212}Po (and ^{214}Po). As already pointed out in Section 2, the only detector part selected for low-radiation background was the optical window. However, the internal background is strongly reduced in the coincidence spectra, as will be demonstrated below.

The coincidence background, measured for a time period of 12.0 d, is shown in Fig. 6. The diagonal band of events arises from 1461 keV

Table 1
Measured singles and coincidence peak efficiencies, η, for ^{22}Na and ^{60}Co point-like calibration sources. The last column shows the simulated coincidence values. The efficiency is defined as the net intensity of a given peak divided by the total number of decaying nuclei during the counting period.

Singles[a]	η_{sing}	Coincidences	η_{coin}	η_{coin}^{sim}
511 (^{22}Na)	0.252 ± 0.013	511, 511 (^{22}Na)	0.124 ± 0.006	0.125 ± 0.003
1786 (^{22}Na)	0.0348 ± 0.0019	511, 1786 (^{22}Na)	0.0515 ± 0.0026	0.0541 ± 0.0019
1332 (^{60}Co)	0.0731 ± 0.008	1172, 1332 (^{60}Co)	0.0264 ± 0.0025	0.0258 ± 0.0011

[a] For detector 1 only.

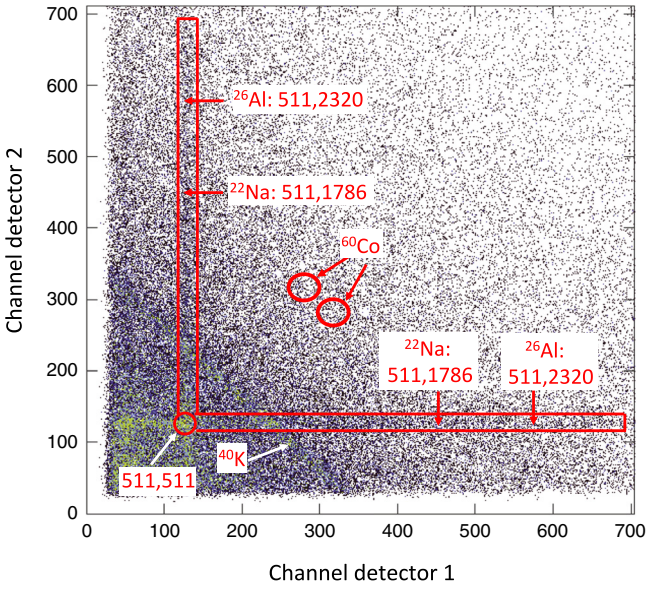

Fig. 6. (Color online) Two-dimensional histogram of energy deposited in detector 2 versus energy deposited in detector 1. The data represent the background obtained without the meteorite fragment (but with the plexiglass sample holder) in place. The running time was about 12.0 d. The diagonal band of events is caused by 1461 keV photons (^{40}K) that Compton scatter from one detector to the other. The horizontal and vertical bands of events at 511 keV originate from positron annihilation after pair production and the decay of ^{208}Tl. The coincidence gates used in the present work for ^{22}Na, ^{26}Al, and ^{60}Co detection are shown as red regions (see text).

photons (^{40}K) that Compton scatter from one detector to the other. The horizontal and vertical bands at 511 keV originate from positron decays after pair production, and from 510.7 keV photons emitted in the decay of ^{208}Tl. The coincidence gates of main interest for the detection of ^{22}Na, ^{26}Al, and ^{60}Co are marked in the figure. The red circle corresponds to 511, 511 coincidences, while the two close red circles refer to 1173, 1332 coincidences (for ^{60}Co). The coincidence gate enclosed by the horizontal and vertical red lines contains events where one counter detects a 511 keV photon. The energy deposition in the other counter is marked by arrows for ^{22}Na and ^{26}Al decays.

The background count rates for these gates, in units of counts per minute (cpm), are listed in Table 2. Our background count rates for 511, 511 and 511, 1786 coincidence events amount to 0.15 cpm and 0.074 cpm, respectively. The first value (0.15 cpm) is lower by a factor of two compared to the result of Povinec [3], who employed NaI(Tl) counters of similar size compared to our detectors. The second value (0.074 cpm) is a factor of four higher than the result of Ref. [3], presumably because their detectors were especially selected for low background. Our background for 511, 511 coincidence events is slightly lower compared to Heusser et al. [11], who also employed NaI(Tl) counters of similar size. However, their coincidence backgrounds for 511, 1786, 511, 2320 and 1173, 1332 events are lower by factors of 2.0, 1.7 and 3.9, respectively. This is explained by their more massive and complex passive shield, detectors that are especially designed for low-level counting, and an active veto (anti-muon) shield.

From the background count rates, we can estimate minimum detectable activities, A_{min}, for ^{22}Na and ^{60}Co point sources. The A_{min} values

Table 2
Measured coincidence background count rates, in units of counts per minute (cpm), and minimum detectable activities (in mBq) for point sources, in the regions of interest for ^{22}Na, ^{26}Al, and ^{60}Co.

Region	Coincidence	BG count rate (cpm)	A_{min} (mBq)[a]
	511, 511	0.15	1.3[b]
^{22}Na	511, 1786	0.074	2.1
^{26}Al	511, 2320	0.037	2.0
^{60}Co	1172, 1332	0.082	4.4

[a] Applicable for a counting time of 12 d.

[b] Based on the decay of ^{22}Na.

are calculated using the expression $A_{min} = N_{min}/(\eta_{coin} t_m)$, with N_{min} the minimum number of net counts (i.e., total minus background) in the region of interest, η_{coin} the coincidence detection efficiency listed in Table 1, and t_m the duration of the background measurement. The quantity N_{min} was estimated from the number of observed background counts in a given coincidence gate using Bayesian inference [12]. The observed total and background counts were modeled according to Poissonian distributions. Several different non-informative priors were tested (uniform, Gaussians with large widths, etc.) and gave similar results. The resulting minimum detectable activities, obtained for a counting period of 12 d, are listed in the last column of Table 2.

Our minimum detectable activity of 1.3 mBq for 511, 511 coincidences, appropriate for the decay of ^{22}Na and a counting period of 12 d, can be compared with previous measurements featuring coincidence efficiencies similar to our setup. Povinec [3] reports a value of 3.7 mBq for a counting time of 28 h, using a $\gamma\gamma$-coincidence spectrometer similar to ours consisting of NaI(Tl) detectors. Zhang et al. [8] report a detection limit of 3 mBq for a counting time of 20 h, employing a $\gamma\gamma$-coincidence spectrometer consisting of two BGO detectors. The present and previous values are in agreement, considering that the minimum detectable activity scales approximately with the square root of the counting period.

3.3. Detector simulations

Monte Carlo simulations of singles and coincidence efficiencies were performed with the Geant4 toolkit, version 9.6 [13]. All components of the setup, including the detectors, the lead plate between them, the passive shielding (copper, steel, lead), and the extended source or sample geometry, were incorporated into the Geant4 model. We defined the simulated detection efficiency in the same manner as the experimental efficiency, i.e., as the ratio of the net intensity of a given peak and the total number of decaying nuclei during the measurement period. Therefore, the simulated efficiency implicitly included the γ-ray branching ratio. Because the simulation had no energy resolution, we convolved the simulated spectrum with an energy dependent Gaussian function before determining the efficiency. The Gaussian function has the same FWHM as the measured peak for the same γ-ray energy.

Twelve million nuclear decays were simulated for ^{22}Na and ^{60}Co, assuming point-source geometries. The simulated coincidence efficiencies are listed in the last column of Table 1. No arbitrary scaling of the simulation results was performed. Measured and simulated coincidence efficiencies agreed within ≈5%.

3.4. Meteorite fragment

The performance of the $\gamma\gamma$-coincidence spectrometer was tested by measuring a fragment of the Farmville meteorite that fell on December 4, 1934, in Pitt County, North Carolina, USA. The meteorite sample (NCSM 44) was obtained from the collection at the North Carolina Museum of Natural Sciences for this study. Properties of the Farmville meteorite have been summarized in Howard et al. [14]. That work reported on the measurement of the cosmogenic ^{26}Al activity in a 569-g fragment of the meteorite using a complex spectrometer consisting of a large volume HPGe detector (135% relative efficiency) and a large 16-segment NaI(Tl) annulus (71-cm diameter × 33-cm length). In the present work, we are measuring a much smaller fragment of the Farmville meteorite, with a mass of 17.7 g, using only two NaI(Tl) detectors.

The radioisotope ^{26}Al has a half-life of $T_{1/2} = (7.17 \pm 0.24) \times 10^5$ yr and decays predominantly by positron emission and electron capture to the first excited state in ^{26}Mg. For 100 decaying ^{26}Al nuclei, 99.76 ± 0.04 photons of 1808.7 keV energy and 163.5 ± 0.4 photons of 511 keV energy are emitted.

The relevant sections of the coincidence spectra are shown in Fig. 7. In the top panel, the spectrum in red was obtained with the meteorite fragment inside the sample holder, while the spectrum in blue refers to the background measurement with the sample holder and no meteorite. Both the sample and the background were counted for about 12 days each. In the meteorite run, an excess of counts was detected in the two energy regions of the characteristic photon of ^{26}Al (1809 keV and 2320 keV = 511 + 1809 keV). The bottom panel shows the difference of the red and blue histograms.

The ^{26}Al activity at the time of meteorite fall, A_0, in units of disintegrations per minute per kilogram (dpm/kg), can be estimated using

$$\frac{A_0}{m} = \frac{I_\gamma^p}{m\,\eta_{coin}^{sim}} \frac{\lambda e^{\lambda t_d}}{(1 - e^{-\lambda t_m})} \tag{1}$$

where $m = 0.0177$ kg is the mass of the fragment, I_γ^{net} is the measured net intensity of the 511, 2320 coincidence peak in Fig. 7, η_{coin}^{sim} is the simulated coincidence efficiency, $\lambda = 3.06334 \times 10^{-14}$ s^{-1} is the ^{26}Al decay constant, $t_d = 2.5826 \times 10^9$ s is the time since meteorite fall, and $t_m = 1.098 \times 10^6$ s is the measurement time. Since our Geant4 model accurately reproduces the coincidence efficiencies measured using the ^{22}Na and ^{60}Co point sources (Table 1), we simulated the coincidence efficiencies for ^{26}Al nuclei decaying inside the meteorite fragment. To this end, we approximated the fragment by a spherical shape, with the radius (1.04 cm) given by the known mass and density (3.73 g/cm^3), assuming that the ^{26}Al nuclei are distributed uniformly throughout the spherical volume. The result was $\eta_{coin}^{sim} = 0.0224 \pm 0.0009$, about a factor of 1.8 lower compared to the value for a ^{26}Al point source. Tests showed that the additional uncertainty introduced by the spherical approximation was negligible in the overall error budget.

We find a value of $A_0/m = 52.9 \pm 7.8$ dpm/kg for the small (17.7 g) fragment measured in the present work. This value agrees with $A_0/m = 48.5 \pm 3.5$ dpm/kg from Howard et al. [14] for a much larger fragment (569 g) of the same meteorite.

4. Summary and conclusions

We discussed the performance of a new low-background spectrometer, based on $\gamma\gamma$-coincidence counting. Measured coincidence efficiencies were in the range of 3% to 12% for two- or three-photon detections in ^{22}Na or ^{60}Co. The coincidence detection technique is of particular interest because it improves significantly the signal-to-background ratio. Our estimated minimum detectable activities, applicable to a counting time of 12 d, amounted to 1–4 mBq for ^{22}Na, ^{26}Al, and ^{60}Co. The spectrometer was simulated using Geant4, and the results were used for estimating coincidence efficiencies for volume sources. The instrument was tested by measuring the concentration of cosmogenic ^{26}Al in a small meteorite fragment (17.7 g), with a result of 52.9 ± 7.8 dpm/kg at the time of meteorite fall. Future work will discuss the usefulness of the device for measuring radium, thorium, and uranium in environmental samples.

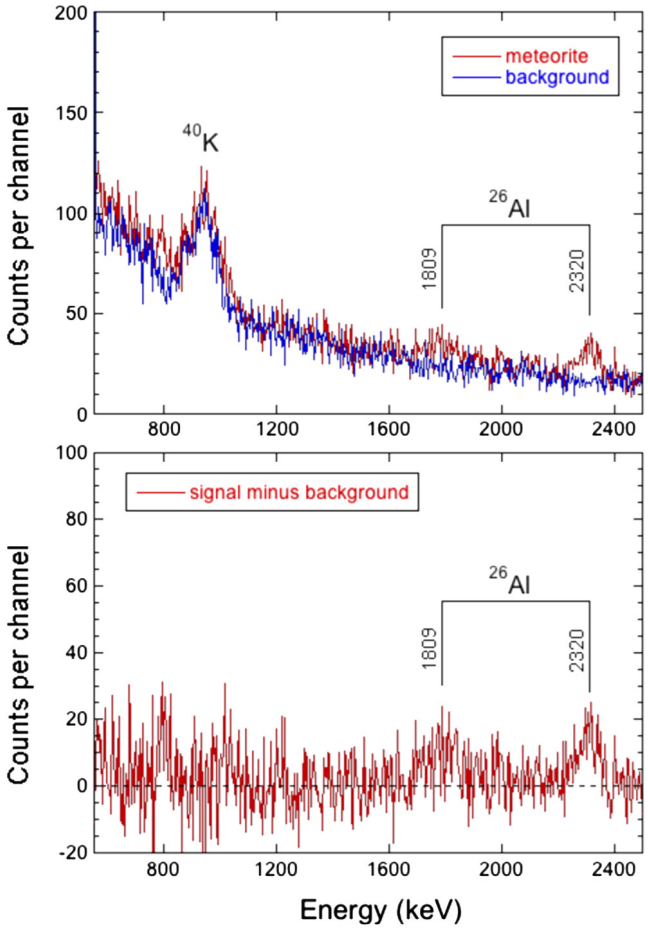

Fig. 7. (Color online) Coincidence spectra for events detected in coincidence with 511 keV photons in one counter (i.e., the gate enclosed by the horizontal and vertical red lines in Fig. 6). The counting time for each run was about 12 d. Top: spectra obtained by measuring a 17.7-g fragment of the Farmville meteorite (red histogram) and the sample holder without the meteorite (blue histogram). In the run with the meteorite, an excess of counts appears in the energy regions of the characteristic photon of ^{26}Al (1809 keV and 2320 keV = 511 + 1809 keV). The peak near 950 keV arises from the diagonal band of Compton-scattered 1461 keV photons (^{40}K) crossing the 511 keV gate shown in red in Fig. 6. Bottom: difference of the red and blue histograms shown in the top panel.

Acknowledgments

We would like to thank Calvin Howell and John Wilkerson for their encouragement. This work was supported in part by the U.S. Department of Energy under Contract No. DE-FG02-97ER41041, and by the Brazil Science Mobility Program (BSMP), Coordenação de Aperfeiçoamento de Pessoal de Nível Superior (CAPES)—Brasil.

References

[1] W. Roedel, On low-level-counting of positron emitters, Nucl. Instrum. Methods 83 (1970) 88–92.

[2] J.A. Cooper, R.W. Perkins, An anticoincidence-shielded dual Ge(Li) gamma-ray spectrometer for low-level environmental radionuclide analysis and gamma-gamma coincidence studies, Nucl. Instrum. Methods 94 (1971) 29–38.

[3] P. Povinec, Dual parameter gamma-ray spectrometer for low-level counting, Isotopenpraxis 18 (1981) 92–95.

[4] R. Grismore, et al., A very-low-level gamma-ray analysis system for modest laboratories, Nucl. Instrum. Methods A 402 (1998) 164–170.

[5] W. Zhang, J. Yi, P. Mekarski, I. Hoffman, K. Ungar, A.-P. Leppänen, A system for low-level the cosmogenic 22Na radionuclide measurement by gamma–gamma coincidence method using BGO detectors, J. Radioanal. Nucl. Chem. 287 (2011) 551–555.
[6] J.L. Burnett, A.V. Davies, Investigating the time resolution of a compact multidimensional gamma-spectrometer, J. Radioanal. Nucl. Chem. 288 (2011) 699–703.
[7] R. Britton, J. Burnett, A. Davies, P.H. Regan, Preliminary simulations of NaI(Tl) detectors, and coincidence analysis using event stamping, J. Radioanaly. Nucl. Chem. 295 (2012) 573–577.
[8] W. Zhang, K. Ungar, M. Stukel, P. Mekarski, A gamma-gamma coincidence/anticoincidence spectrometer for low-level cosmogenic $^{22}Na/^{7}Be$ activity ratio measurement, J. Environ. Radioact. 130 (2014) 1–6.
[9] K.B. Swartz, D.W. Visser, J.M. Baris, A Java-based data acquisition system for nuclear physics, Nucl. Instrum. Methods A 463 (2001) 354–360.
[10] P. Theodorsson, K/Th/U in photomultiplier tubes and improved low-level NaI detectors, Nucl. Instrum. Methods A 506 (2003) 143–148.
[11] G. Heusser, et al., Conditions of the cosmic ray exposure of the Jilin chondrite, Earth Planet. Sci. Lett. 72 (1985) 263–272.
[12] S. Andreon, B. Weaver, Bayesian Methods for the Physical Sciences, Springer International Publishing, 2015.
[13] S. Agostinelli, et al. (Geant4 Collaboration), Geant4-a simulation toolkit, Nucl. Instrum. Methods A 506 (2003) 250–303 version `Geant4.8.1-p1`.
[14] C. Howard, M. Ferm, J. Cesaratto, S. Daigle, C. Iliadis, Radioisotope studies of the farmville meteorite using $\gamma\gamma$-coincidence spectrometry, Appl. Radiat. Isot. 94 (2014) 23–29.